Inorg. Chem. **2005**, *44*, 7063–7069

Cyano-Bridged $Cu^{II}-M^{V}$ (M = Mo, W) Bimetallic Layered Complexes Exhibiting Novel Honeycomblike Structures

Young Sin You,[†] Jung Hee Yoon,[†] Jeong Hak Lim,[†] Hyoung Chan Kim,[‡] and Chang Seop Hong*,[†]

Department of Chemistry and Center for Electro- and Photo-Responsive Molecules, Korea University, Seoul 136-701, Korea, and Material Science Laboratory, Korea Basic Science Institute, Daejeon 305-333, Korea

Received April 26, 2005

Self-assembly of a new precursor $[Cu(L)](ClO_4)_2$ (**1**) (L = macrocyclic ligand) with octacyanometalates $[M(CN)_8]^{3-}$ (M = Mo, W) produced two-dimensional cyano-bridged Cu(II)–M(V) bimetallic assemblies $[Cu(L)]_{3n}[M(CN)_8]_{2n}\cdot 6nH_2O$ [M = Mo (**2**), W (**3**)] with novel honeycomblike structures, characterized by spectroscopic data, single-crystal X-ray diffraction studies, and magnetic measurements. The crystallographic determination reveals that compounds **2** and **3** are isostructural and crystallize in the triclinic system ($P\bar{1}$). The Cu atom in a distorted octahedral environment experiences a tetragonal elongation of apical nitrogen atoms exhibiting average $Cu-N_{ax}$ lengths of 2.566 Å for **2** and 2.593 Å for **3**, which accounts for the Jahn–Teller effect of a Cu(II) ion. The Cu–NC angles are magnetically important, ranging from 135.7 to 159.2°. Three types of L in the crystal lattice are observed, which are dependent on the relative positions of the pendant hydroxyl groups with respect to the CuN_4 basal plane. The positions are correlated with hydrogen bonding of OH groups to neighboring atoms. The magnetic data indicate that ferromagnetic and antiferromagnetic interactions between Cu(II) and M(V) through the CN linkage coexist.

Introduction

Molecule-based magnetic materials have attracted much attention from potential applications to magnetic devices.[1] In recent years hybrid magnetic materials including chiral magnets,[2−4] photomagnets,[5−7] and molecular magnetic conductors[8] have been actively studied to open a new opportunity in molecular magnetism. Hexacyanometalates $[M(CN)_6]^{n-}$ (M = Cr, Mn, Fe, Co, etc.) have been utilized as good building blocks for the fabrication of molecular bimetallic systems with various structures such as heteropolynuclear, 1D chain, 2D layer, and 3D network entities.[9−12] Particularly, among them, 2D honeycomblike structures are attractive from an aesthetical and magnetic point of view.[13−15] In fact, several other compounds with honeycomb structures have been synthesized and characterized structurally and magnetically by choosing bridging ligands such as oxalate, azide, and 2,2′-bipyrimidine.[16−18]

* To whom correspondence should be addressed. E-mail: cshong@korea.ac.kr.
[†] Korea University.
[‡] Korea Basic Science Institute.

(1) Turnbull, M. M.; Sugimoto, T.; Thompson, L. K. *Molecule-Based Magnetic Materials*; American Chemical Society: Washington, DC, 1996.
(2) Inoue, K.; Kikuchi, K.; Ohba, M.; Okawa, H. *Angew. Chem., Int. Ed.* **2003**, *42*, 4709.
(3) Inoue, K.; Imai, H.; Ghalsasi, P. S.; Kikuchi, K.; Ohba, M.; Okawa, H.; Yakhmi, J. V. *Angew. Chem., Int. Ed.* **2001**, *40*, 4242.
(4) Coronado, E.; Galan-Mascaros, J. R.; Gomez-Garcia, C. J.; Martinez-Agudo, J. M. *Inorg. Chem.* **2001**, *40*, 113.
(5) Sato, O. *Acc. Chem. Res.* **2003**, *36*, 9692.
(6) (a) Arimoto, Y.; Ohkoshi, S.; Zhong, Z. J.; Seino, H.; Mizobe, Y.; Hashomoto, K. *J. Am. Chem. Soc.* **2003**, *125*, 9240. (b) Li, G.; Akitsu, T.; Sato, O.; Einaga, Y. *J. Am. Chem. Soc.* **2000**, *125*, 12396.
(7) (a) Herrera, J. M.; Marvaud, V.; Verdaguer, M.; Marrot, J.; Kalisz, M.; Mathonière, C. *Angew. Chem., Int. Ed.* **2004**, *43*, 5467. (b) Dei, A. *Angew. Chem., Int. Ed.* **2005**, *44*, 1160. (c) Rombaut, G.; Verelst, M.; Golhen, S.; Ouahab, L.; Mathonière, C.; Kahn, O. *Inorg. Chem.* **2001**, *40*, 1151.
(8) Coronado, E.; Galan-Mascaros, J. R.; Gomez-Garcia, C. J.; Laukhin, V. *Nature* **2000**, *408*, 447.
(9) Marvaud, V.; Decroix, C.; Scuiller, A.; Tuyeras, F.; Guyard-Duhayon, C.; Vaissermann, J.; Marrot, J.; Gonnet, F.; Verdaguer, M. *Chem.—Eur. J.* **2003**, *9*, 1692.
(10) Colacio, E.; Dominguez-Vera, J. M.; Ghazi, M.; Kivekas, R.; Klinga, M.; Moreno, J. M. *Chem. Commun.* **199**8, 1071.
(11) Kou, H.-Z.; Zhou, B. C.; Gao, S.; Liao, D.-Z.; Wang, R.-L. *Inorg. Chem.* **2003**, *42*, 5604.
(12) Kou, H.-Z.; Gao, S.; Zhang, J.; Wen, G.-H.; Su, G.; Zheng, R. K.; Zhang, X. X. *J. Am. Chem. Soc.* **2001**, *123*, 11809.
(13) Kou, H.-Z.; Gao, S.; Bai, O.; Wang, Z.-M. *Inorg. Chem.* **2001**, *40*, 6287.
(14) Ohba, M.; Okawa, H.; Fukita, N.; Hashimoto, Y. *J. Am. Chem. Soc.* **1997**, *119*, 1011.
(15) Hong, C. S.; You, Y. S. *Inorg. Chim. Acta* **2004**, *357*, 3271.
(16) Pellaux, R.; Schmalle, H. W.; Huber, R.; Fischer, P.; Hauss, T.; Ouladdiaf, B.; Decurtins, S. *Inorg. Chem.* **1997**, *36*, 2301.

10.1021/ic050634c CCC: $30.25
Published on Web 09/01/2005

To develop a new class of molecule-based magnetic materials there has been intensive interest in employing octacyanometalates $[M(CN)_8]^{n-}$ (M = 4d or 5d metal ions) as useful molecular precursors on account of their diffuse orbitals, diverse coordination fashions, and photoresponsive properties.[19] A variety of structures with these building bricks have been successfully attained, for instance, spanning from discrete molecules, one-dimensional (1D) chains, and 2D sheets to 3D networks.[20,21] Most of them are octacyanotungstate(V)-based bimetallic assemblies possessing salient magnetic and other properties.[20,22] In contrast, there exist only a few examples of octacyanomolybdate(V)-based complexes such as high-spin clusters, 1D chains with moniliform structure, and a 2D coordination polymer.[21] Moreover, the understanding of the exchange coupling mechanism between magnetic centers in such compounds remains subject to one of the current issues to get insights into 3d−4d (5d) magnetic systems.[23] In this line, a new 1D cyano-bridged Cu(II)−Mo(V) compound with a rope-ladder chain structure, in which the Cu ion is surrounded by a simple macrocyclic ligand cyclam (cyclam = 1,4,8,11-tetraazacyclotetradecane) was reported.[24] To explore structural feasibility in octacyanometalate(V)-based 3d−4d (5d) systems, we have attempted to devise some bimetallic assemblies with new structural patterns and magnetic natures by varying macrocyclic ligands.

Herein we present the syntheses, structures, and magnetic properties of unprecedented 2D layered Cu(II)−M(V) complexes $[Cu(L)]_{3n}[M(CN)_8]_{2n}\cdot 6nH_2O$ (M = Mo (**2**), W (**3**); L = macrocyclic ligand) with honeycomblike structures, formed by self-assembling $[Cu(L)]^{2+}$ (**1**) and $[M(CN)_8]^{3-}$ in a ratio of 3:2. It deserves to be noted that the prepared compounds with honeycomblike frameworks exhibit the first structural types found in the octacyanometalate(V)-based bimetallic series. Temperature- and field-dependent magnetic features demonstrate that paramagnetic Cu(II) and M(V) centers are ferromagnetically and antiferromagnetically coupled through cyanide bridges.

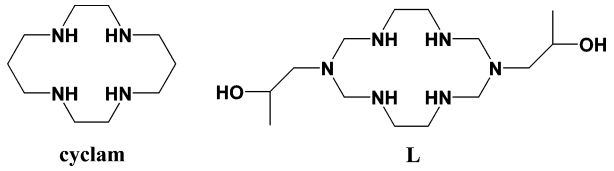

Experimental Section

Reagents. All chemicals and solvents in the synthesis were of reagent grade and used as received. All manipulations were performed under aerobic conditions.

Synthesis. ***Caution!*** *Perchlorate salts of metal compounds with organic ligands are potentially explosive. Only small amounts of material should be cautiously handled.*

$[Cu(L)](ClO_4)_2$ (1). To a methanolic solution (75 mL) of $CuCl_2\cdot 6H_2O$ (8.6 g) with vigorous stirring was slowly added ethylenediamine (99%, 6.8 mL) by syringe for 20 min. After 10 min of stirring, addition of paraformaldehyde (10 g) and 1-amino-2-propanol (93%, 17 mL) followed. The mixture was refluxed for 12 h and then filtered hot. To the filtrate was added $LiClO_4$ (4.9 g), and an yellow-orange powder formed. The precipitate was washed with methanol and dried in air. The solid was dissolved in a minimum amount of DMF and recrystallized by diffusing ether vapor into the DMF solution to give crystalline solids in a yield of 60%. Anal. Calcd for $C_{14}H_{34}Cl_2CuN_6O_{10}$: C, 29.0; H, 5.90; N, 14.5. Found: C, 29.0; H, 6.11; N, 14.6.

$[Cu(L)]_{3n}[Mo(CN)_8]_{2n}\cdot 6nH_2O$ (2). To $[Cu(L)](ClO_4)_2$ (0.15 mmol) dissolved in $MeCN/H_2O$ (5:1) was added a methanolic solution of $(Bu_4N)_3[Mo(CN)_8]$ (0.10 mmol) with stirring in the dark (pH ≈ 6.5) to avoid photoreduction. The filtered solution was left undisturbed in the dark, forming pale brown crystals in a yield of 54%. Anal. Calcd for $C_{58}H_{114}Cu_3Mo_2N_{34}O_{12}$: C, 37.4; H, 6.17; N, 25.6. Found: C, 37.2; H, 6.15; N, 25.6.

$[Cu(L)]_{3n}[W(CN)_8]_{2n}\cdot 6nH_2O$ (3). In the dark a methanolic solution of $(Bu_4N)_3[W(CN)_8]$ (0.10 mmol) was added to $[Cu(L)](ClO_4)_2$ (0.15 mmol) dissolved in DMF (pH ≈ 6.5). After being stirred for a few minutes, the resulting solution was filtered. The filtrate was allowed to stand undisturbed in the dark, giving brown crystals in a yield of 60%. Anal. Calcd for $C_{58}H_{114}Cu_3N_{34}O_{12}W_2$: C, 34.2; H, 5.64; N, 23.4. Found: C, 34.0; H, 5.58; N, 23.7.

Physical Measurements. Elemental analyses for C, H, and N were performed at the Elemental Analysis Service Center of Sogang University. Infrared spectra were obtained from KBr pellets with a Bomen MB-104 spectrometer. Magnetic susceptibilities for **2** and **3** were carried out using a Quantum Design MPMS-7 SQUID susceptometer. Diamagnetic corrections of **2** and **3** were estimated from Pascal's tables.

Crystallographic Structure Determination. X-ray data for **2** and **3** were collected on a Bruker SMART APEXII diffractometer equipped with graphite-monochromated Mo Kα radiation (λ = 0.710 73 Å). Reflection data were corrected for Lorentz and polarization factors. The structures were solved by direct methods and refined by full-matrix least-squares analysis using anisotropic thermal parameters for non-hydrogen atoms with the SHELXTL program.[25] All hydrogen atoms except for hydrogens bound to water molecules were calculated at idealized positions and refined by use

(17) De Munno, G.; Julve, M.; Viau, G.; Lloret, F.; Faus, J.; Viterbo, D. *Angew. Chem., Int. Ed. Engl.* **1996**, *35*, 1807.
(18) De Munno, G.; Julve, M.; Nicolo, F.; Lloret, F.; Fasu, J.; Ruiz, R.; Sinn, E. *Angew. Chem., Int. Ed. Engl.* **1993**, *32*, 613.
(19) (a) Zhong, Z. J.; Seino, H.; Mizobe, Y.; Hidai, M.; Fujishima, A.; Ohkosh, S.-i.; Hashimoto, K. *J. Am. Chem. Soc*. **2000**, *122*, 2952. (b) Pradhan, R.; Desplanches, C.; Guionneau, P.; Sutter, J.-P. *Inorg. Chem.* **2003**, *42*, 6607. (c) Bennett, M. V.; Long, J. R. *J. Am. Chem. Soc.* **2003**, *125*, 2394.
(20) (a) Li, D.; Zheng, L.; Zhang, Y.; Huang, J.;. Gao, S; Tang, W. *Inorg. Chem.* **2003**, *42*, 6123. (b) Ohkoshi, S.-i.; Arimoto, Y.; Hozumi, T.; Seino, H.; Mizobe, Y.; Hashomoto, K. *Chem. Commun.* **2003**, 2772. (c) Podgajny, R.; Korzeniak, T.; Balanda, M.; Wasiutynski, T.; Errington, W.; Kemp, T. J.; Alcock, N. W.; Sieklucka, B. *Chem. Commun.* **2002**, 1138. (d) Korzeniak, T.; Stadnicka, K.; Rams, M.; Sieklucka, B. *Inorg. Chem.* **2004**, *43*, 4811.
(21) (a) Larionova, J.; Gross, M.; Pilkington, M.; Andres, H.; Stoeckli-Evans, H.; Gudel, H. U.; Decurtins, S. *Angew. Chem., Int. Ed.* **2000**, *39*, 1605. (b) Bonadio, F.; Gross, M.; Stoeckli-Evans, H.; Decurtins, S. *Inorg. Chem.* **2002**, *41*, 5891. (c) Li, D.-f.; Gao, S.; Zheng, L.-m.; Tang, W.-x. *J. Chem. Soc., Dalton Trans.* **2002**, 2805. (d) Korzeniak, T.; Podgajny, R.; Alcock, N. W.; Lewinski, K.; Balanda, M.; Wasiutynski, T.; Sieklucka, B. *Polyhedron* **2003**, *22*, 2183.
(22) (a) Kashiwagi, T.; Ohkoshi, S.-i.; Seino, H.; Mizobe, Y.; Hashimoto, K. *J. Am. Chem. Soc.* **2004**, *126*, 5024. (b) Arimoto, Y.; Ohkoshi, S.-i.; Zhong, Z. J.; Seino, H.; Mizobe, Y.; Hashimoto, K. *J. Am. Chem. Soc.* **2003**, *125*, 9240.
(23) Chibotaru, L. F.; Mironov, V. S.; Ceulemans, A. *Angew. Chem., Int. Ed.* **2001**, *40*, 4429.
(24) You, Y. S.; Kim, D.; Do, Y.; Oh, S. J.; Hong, C. S. *Inorg. Chem.* **2004**, *43*, 6899.
(25) Sheldrick, G. M. *SHELXTL*, version 5; Bruker AXS: Madison, WI, 1995.

Table 1. Crystallographic Data for **2** and **3**

param	**2**	**3**
formula	$C_{29}H_{57}Cu_{1.5}MoN_{17}O_6$	$C_{29}H_{57}Cu_{1.5}N_{17}O_6W$
fw	931.17	1019.08
cryst system	triclinic	triclinic
space group	$P\bar{1}$	$P\bar{1}$
temp (K)	100	100
a (Å)	8.9692(3)	9.0220(5)
b (Å)	15.1424(5)	15.2639(9)
c (Å)	15.7846(5)	15.8160(9)
α (deg)	69.8190(10)	69.520(2)
β (deg)	86.0370(10)	85.966(2)
γ (deg)	89.0550(10)	89.063(2)
V (Å^3)	2007.30(11)	2035.2(2)
Z	2	2
d_{calc} (g cm^{-3})	1.541	1.663
μ (mm^{-1})	1.162	3.662
F(000)	967	1031
θ range (deg)	1.38−28.31	1.38−30.59
reflcns collcd	33 170	34 817
unique reflcns	9806	11 942
no. of params	502	496
R1[a] [$I > 2\sigma(I)$]	0.0584	0.0431
wR2[b] [$I > 2\sigma(I)$]	0.1355	0.0957
largest resids (e Å^{-3})	1.644/−1.007	1.059/−1.382

[a] $R1 = \Sigma||F_o| - |F_c||/\Sigma|F_c|$. [b] $wR2 = [\Sigma w(F_o^2 - F_c^2)^2/\Sigma w(F_o^2)^2]^{1/2}$.

of the riding models. Crystallographic data and details of data collection are listed in Table 1.

Results and Discussion

Synthesis and Characterization. The Cu(II) complex (**1**) with the macrocyclic ligand L was prepared by the template condensation reaction routes in the presence of appropriate reagents. The IR data exhibit OH stretchings of hydroxyl pendant groups at 3522 s cm^{-1}. For secondary amines, NH stretchings appear at 3256 s and 3299 s cm^{-1}, implying that the lower NH peaks arise from hydrogen bonding with hydroxyl groups and perchlorate anions. The existence of perchlorate anions is detected as strong multiple peaks in the IR spectra in the range 1128−1064 cm^{-1}.

The synthesis of compounds **2** and **3** was carried out self-assembling $[Cu(L)]^{2+}$ and $[M(CN)_8]^{3-}$ in a stoichiometric ratio of 3:2. The axial vacant sites of $[Cu(L)]^{2+}$ are able to be occupied by the N ends of CN ligands among the precursor $[M(CN)_8]^{3-}$, resulting in neutral coordination polymers of **2** and **3**. The most conspicuous features of the IR spectra concern the existence of 2143 m, 2135 m (sh) cm^{-1} for **2** and 2147 m, 2135 m cm^{-1} for **3**, which are assigned to characteristic CN stretching vibrations. When compared with CN peaks centered at 2140 m, 2123 m cm^{-1} for $(Bu_4N)_3Mo(CN)_8$ and 2141 m, 2130 m, 2123 m (sh) cm^{-1} for $(Bu_4N)_3W(CN)_8$, the shift toward higher frequencies suggests the advent of bridging cyanide in the complexes, indicating the formation of coordination compounds bridged by CN groups among the $[M(CN)_8]^{3-}$ precursors. The positions of the OH peaks move down to the lower frequencies of 3423 cm^{-1} (**2**) and 3429 cm^{-1} (**3**), implying that hydrogen bonding is present in the lattice. The secondary amines also experience hydrogen bonding, which accounts for the shift of NH stretchings toward lower frequencies of 3248 s, 3217 s cm^{-1} for **2** and 3248 s, 3219 s cm^{-1} for **3**.

Description of the Structures. $[Cu(L)]_{3n}[M(CN)_8]_{2n}\cdot 6nH_2O$ (M = Mo (2), W (3)). Figure 1 illustrates the perspective molecular view of **2** with selected atom-numbering scheme. Compounds **2** and **3** are isostructural and crystallize in the triclinic system ($P\bar{1}$). Selected bond distances and angles of **2** and **3** are listed in Tables 2 and 3, respectively. Each asymmetric unit of **2** and **3** is composed of one $[M(CN)_8]^{3-}$ (M = Mo, W) anion and three half $[Cu(L)]^{2+}$ cations. The environment around M can be viewed as distorted square antiprismatic, comprising eight CN groups

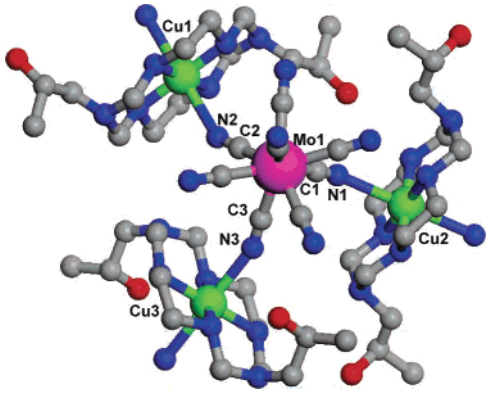

Figure 1. Molecular view of **2** where C is presented in gray, N in blue, O in red, Cu in green, and Mo in pink.

Table 2. Bond Lengths (Å) and Angles (deg) for **2**[a]

Mo(1)−C(1)	2.149(5)	Mo(1)−C(5)	2.154(5)
Mo(1)−C(2)	2.158(5)	Mo(1)−C(8)	2.160(5)
Mo(1)−C(7)	2.160(5)	Mo(1)−C(6)	2.165(5)
Mo(1)−C(3)	2.166(5)	Mo(1)−C(4)	2.167(5)
Cu(1)−N(10)	2.007(4)	Cu(1)−N(9)	2.012(4)
Cu(1)−N(2)	2.566(4)	Cu(2)−N(12)	1.999(5)
Cu(2)−N(13)	2.013(4)	Cu(2)−N(1)	2.583(5)
Cu(3)−N(15)	2.002(4)	Cu(3)−N(16)	2.032(4)
Cu(3)−N(3)	2.548(5)		
C(1)−Mo(1)−C(5)	97.50(17)	C(1)−Mo(1)−C(2)	79.40(17)
C(5)−Mo(1)−C(2)	144.07(17)	C(1)−Mo(1)−C(8)	88.49(19)
C(5)−Mo(1)−C(8)	144.67(18)	C(2)−Mo(1)−C(8)	71.26(18)
C(1)−Mo(1)−C(7)	69.63(18)	C(5)−Mo(1)−C(7)	76.06(17)
C(2)−Mo(1)−C(7)	133.10(17)	C(8)−Mo(1)−C(7)	73.55(17)
C(1)−Mo(1)−C(6)	142.58(18)	C(5)−Mo(1)−C(6)	76.93(18)
C(2)−Mo(1)−C(6)	126.16(18)	C(8)−Mo(1)−C(6)	77.4(2)
C(7)−Mo(1)−C(6)	73.16(18)	C(1)−Mo(1)−C(3)	74.60(17)
C(5)−Mo(1)−C(3)	70.44(17)	C(2)−Mo(1)−C(3)	74.30(17)
C(8)−Mo(1)−C(3)	143.85(18)	C(7)−Mo(1)−C(3)	126.37(17)
C(6)−Mo(1)−C(3)	133.93(18)	C(1)−Mo(1)−C(4)	145.82(18)
C(5)−Mo(1)−C(4)	90.83(17)	C(2)−Mo(1)−C(4)	74.68(18)
C(8)−Mo(1)−C(4)	103.56(19)	C(7)−Mo(1)−C(4)	144.33(18)
C(6)−Mo(1)−C(4)	71.59(18)	C(3)−Mo(1)−C(4)	77.19(18)
N(1)−C(1)−Mo(1)	176.2(4)	N(2)−C(2)−Mo(1)	176.7(4)
N(3)−C(3)−Mo(1)	177.9(4)	N(4)−C(4)−Mo(1)	175.8(5)
N(5)−C(5)−Mo(1)	178.2(4)	N(6)−C(6)−Mo(1)	179.0(5)
N(7)−C(7)−Mo(1)	175.2(4)	N(8)−C(8)−Mo(1)	177.3(5)
N(10)−Cu(1)−N(10)$^{\#1}$	180.0(2)	N(10)−Cu(1)−N(9)	86.02(16)
N(10)$^{\#1}$−Cu(1)−N(9)	93.98(16)	N(10)−Cu(1)−N(9)$^{\#1}$	93.98(16)
N(10)$^{\#1}$−Cu(1)−N(9)$^{\#1}$	86.02(16)	N(9)−Cu(1)−N(9)$^{\#1}$	180.0(2)
C(10)−N(9)−Cu(1)	106.6(3)	C(9)−N(9)−Cu(1)	114.0(3)
C(11)−N(10)−Cu(1)	107.0(3)	C(12)−N(10)−Cu(1)	115.0(3)
N(12)$^{\#2}$−Cu(2)−N(12)	180.0(2)	N(12)$^{\#2}$−Cu(2)−N(13)$^{\#2}$	93.50(18)
N(12)−Cu(2)−N(13)$^{\#2}$	86.50(18)	N(12)$^{\#2}$−Cu(2)−N(13)	86.50(18)
N(12)−Cu(2)−N(13)	93.50(18)	N(13)$^{\#2}$−Cu(2)−N(13)	180.000(1)
C(17)−N(12)−Cu(2)	116.1(3)	C(16)−N(12)−Cu(2)	106.6(3)
C(22)−N(13)−Cu(2)	106.3(3)	C(21)−N(13)−Cu(2)	114.2(3)
N(15)$^{\#3}$−Cu(3)−N(15)	180.000(1)	N(15)$^{\#3}$−Cu(3)−N(16)$^{\#3}$	93.67(17)
N(15)−Cu(3)−N(16)$^{\#3}$	86.33(17)	N(15)$^{\#3}$−Cu(3)−N(16)	86.33(17)
N(15)−Cu(3)−N(16)	93.67(17)	N(16)$^{\#3}$−Cu(3)−N(16)	180.000(1)
C(23)−N(15)−Cu(3)	107.2(3)	C(24)−N(15)−Cu(3)	114.8(3)
C(29)−N(16)−Cu(3)	105.8(3)	C(28)−N(16)−Cu(3)	114.6(3)

[a] Symmetry transformations used to generate equivalent atoms: (#1) $-x, -y, -z + 1$; (#2) $-x + 2, -y + 1, -z$; (#3) $-x, -y + 2, -z$.

Table 3. Bond Lengths (Å) and Angles (deg) for **3**[a]

W(1)−C(1)	2.154(6)	W(1)−C(8)	2.156(5)
W(1)−C(6)	2.167(5)	W(1)−C(7)	2.163(5)
W(1)−C(4)	2.167(5)	W(1)−C(3)	2.169(5)
W(1)−C(5)	2.170(5)	W(1)−C(2)	2.177(5)
Cu(1)−N(11)	2.007(4)	Cu(1)−N(9)	2.008(4)
Cu(1)−N(2)	2.600(4)	Cu(2)−N(14)	1.994(4)
Cu(2)−N(12)	1.996(4)	Cu(2)−N(1)	2.607(6)
Cu(3)−N(15)	1.997(4)	Cu(3)−N(17)	2.028(4)
Cu(3)−N(3)	2.570(6)		
C(1)−W(1)−C(8)	89.8(2)	C(1)−W(1)−C(6)	142.94(19)
C(8)−W(1)−C(6)	77.0(2)	C(1)−W(1)−C(7)	145.31(18)
C(8)−W(1)−C(7)	102.4(2)	C(6)−W(1)−C(7)	71.75(19)
C(1)−W(1)−C(4)	97.02(19)	C(8)−W(1)−C(4)	144.82(18)
C(6)−W(1)−C(4)	76.92(19)	C(7)−W(1)−C(4)	91.35(19)
C(1)−W(1)−C(3)	74.64(19)	C(8)−W(1)−C(3)	143.79(18)
C(6)−W(1)−C(3)	133.5(2)	C(7)−W(1)−C(3)	76.59(19)
C(4)−W(1)−C(3)	70.69(16)	C(1)−W(1)−C(5)	69.97(18)
C(8)−W(1)−C(5)	73.71(19)	C(6)−W(1)−C(5)	73.10(19)
C(7)−W(1)−C(5)	144.55(18)	C(4)−W(1)−C(5)	76.37(18)
C(3)−W(1)−C(5)	127.38(18)	C(1)−W(1)−C(2)	78.65(19)
C(8)−W(1)−C(2)	71.23(18)	C(6)−W(1)−C(2)	126.95(19)
C(7)−W(1)−C(2)	74.99(19)	C(4)−W(1)−C(2)	143.95(17)
C(3)−W(1)−C(2)	73.70(17)	C(5)−W(1)−C(2)	132.37(18)
N(1)−C(1)−W(1)	175.0(5)	N(2)−C(2)−W(1)	176.1(5)
N(3)−C(3)−W(1)	178.0(4)	N(4)−C(4)−W(1)	179.3(5)
N(5)−C(5)−W(1)	176.0(4)	N(6)−C(6)−W(1)	179.2(5)
N(7)−C(7)−W(1)	176.4(5)	N(8)−C(8)−W(1)	177.9(5)
N(11)−Cu(1)−N(11)$^{\#1}$	180.0(3)	N(11)−Cu(1)−N(9)$^{\#1}$	94.07(17)
N(11)$^{\#1}$−Cu(1)−N(9)$^{\#1}$	85.93(17)	N(11)−Cu(1)−N(9)	85.93(17)
N(11)$^{\#1}$−Cu(1)−N(9)	94.07(17)	N(9)$^{\#1}$−Cu(1)−N(9)	180.0(4)
C(9)−N(9)−Cu(1)	114.5(3)	C(15)−N(9)−Cu(1)	106.5(3)
C(13)−N(11)−Cu(1)	114.3(3)	C(14)−N(11)−Cu(1)	106.2(3)
N(14)−Cu(2)−N(14)$^{\#2}$	180.0(2)	N(14)−Cu(2)−N(12)$^{\#2}$	86.40(18)
N(14)$^{\#2}$−Cu(2)−N(12)$^{\#2}$	93.60(18)	N(14)−Cu(2)−N(12)	93.60(18)
N(14)$^{\#2}$−Cu(2)−N(12)	86.40(18)	N(12)$^{\#2}$−Cu(2)−N(12)	180.0(3)
C(16)−N(12)−Cu(2)	115.7(3)	C(22)−N(12)−Cu(2)	107.4(3)
C(20)−N(14)−Cu(2)	115.2(3)	C(21)−N(14)−Cu(2)	106.8(3)
N(15)−Cu(3)−N(15)$^{\#3}$	180.0(2)	N(15)−Cu(3)−N(17)	93.67(18)
N(15)$^{\#3}$−Cu(3)−N(17)	86.33(18)	N(15)−Cu(3)−N(17)$^{\#3}$	86.33(18)
N(15)$^{\#3}$−Cu(3)−N(17)$^{\#3}$	93.67(18)	N(17)−Cu(3)−N(17)$^{\#3}$	180.0(2)
C(29)−N(15)−Cu(3)	107.1(3)	C(23)−N(15)−Cu(3)	115.9(3)
C(28)−N(17)−Cu(3)	106.4(3)	C(27)−N(17)−Cu(3)	113.9(3)

[a] Symmetry transformations used to generate equivalent atoms: (#1) $-x+2, -y, -z$; (#2) $-x, -y+1, -z+1$; (#3) $-x+2, -y, -z+1$.

with average M−C bond distances of 2.160(6) Å for **2** and 2.166(8) Å for **3**. The bridging M−C−N angles remain almost linear with the maximum deviation from linearity of 3.8° for **2** and 5° for **3**. These are in the normal range of ocatacyanometalate-based bimetallic systems.[20−24] The adjacent Cu(II) ions are connected to the M(V) center through the three CN bridges with distances of 5.565 Å for Mo1−Cu1, 5.409 Å for Mo1−Cu2, and 5.767 Å for Mo1−Cu3, slightly shorter than those of 5.607 Å for W1−Cu1, 5.438 Å for W1−Cu2, and 5.790 Å for W1−Cu3. The three Cu atoms in the asymmetric unit of **2** are located at the special positions (Cu1, 0, 0, 1/2; Cu2, 1, 1/2, 0; Cu3, 0, 1, 0) whereas those in **3** with the identical asymmetric unit lie at different positions (Cu1, 1, 0, 0; Cu2, 0, 1/2, 1/2; Cu3, 1, 0, 1/2). Each Cu atom with an inversion center adopts a distorted octahedral geometry, as characterized by a tetragonal elongation of apical nitrogen atoms exhibiting Cu−N_{ax} lengths of Cu1−N2 = 2.566 Å, Cu2−N1 = 2.583 Å, Cu3−N3 = 2.548 Å for **2** and of Cu1−N2 = 2.599 Å, Cu2−N1 = 2.607 Å, and Cu3−N3 = 2.572 Å for **3**. This structural distortion is essentially associated with the Jahn−Teller effect of a Cu(II) ion. Each basal plane is composed of four equatorial nitrogen atoms from L with an average Cu−N_{eq} distance of

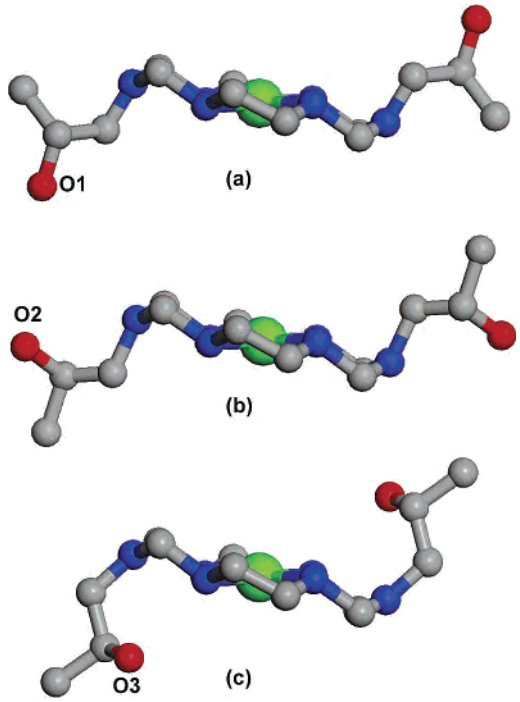

Figure 2. Structural diversity of L showing (a) type I with *S,S*-configuration of the pendant tertiary carbon atoms, (b) type II with *R,R*-configuration of the pendant tertiary carbon atoms, and (c) type III with *S,S*-configuration of the pendant tertiary carbon atoms where the oxygen atoms are positioned closer to the CuN_4 basal plane than those of type I.

2.01(1) Å for both compounds. For **2**, the angles of Cu−NC are different, being 143.7° for Cu1−N2−C2, 135.7° for Cu2−N1−C1, and 157.8° for Cu3−N3−C3. In comparison, the corresponding Cu−NC angles in **3** are a little more obtuse, 144.2° for Cu1−N2−C2, 137.4° for Cu2−N1−C1, and 159.2° for Cu3−N3−C3. It is noted that the angles for Cu1 and Cu2 are much more acute than that for Cu3, which are magnetically important together with the Cu−N_{ax} bond lengths.

It is worthy of noting that the structural variety of the macrocycle L in **2** is 3-fold depending on the positions of the pendant hydroxyl groups with respect to the CuN_4 basal plane (Figure 2). In type I, the tertiary carbon atoms of the two pendant groups represent an *S,S*-configuration and the oxygen atoms (O1) reside away from the basal plane. No hydrogen bonding is observed for the oxygen atoms (O1). The overall molecular shape of type II is identical with that of type I except for the absolute *R,R*-configuration of the tertiary carbon atoms. The oxygen atoms (O2) are located closer to the basal plane and hydrogen-bonded to lattice water molecules and secondary amines of L with distances ranging from 2.764 to 3.066 Å. A conformational isomer of type I is found in type III with *S,S*-configuration of the carbon atoms. The conformer is realized by rotating the −CH(OH)-CH_3 group toward the basal plane and stabilized due to the presence of hydrogen bonding of the oxygen atom (O3) with the N end (N5a; $a = 2 - x, -y, -z$) of the free CN group with a distance of 2.868 Å. Additional hydrogen bonds with secondary amines of L are formed, their lengths spanning from 2.851 to 3.030 Å. It appears that this molecular environment in type III allows the largest bond angle of

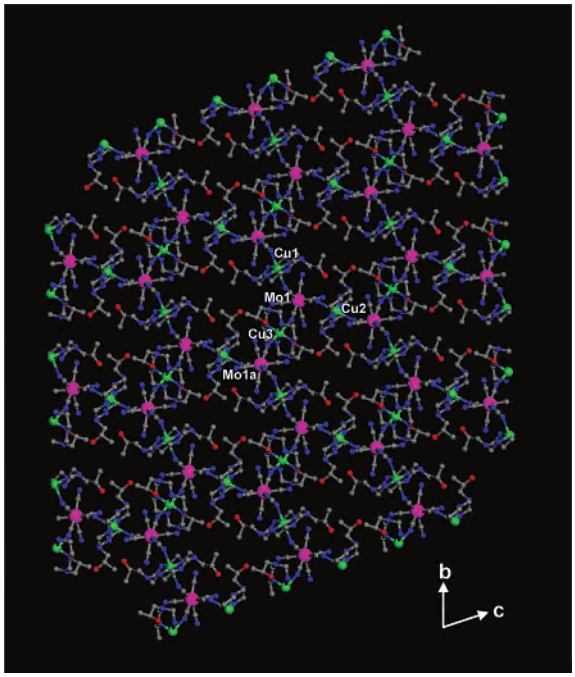

Figure 3. 2D extended layer structure of **2** in the bc plane. Symmetry code: (a) $2 - x, -y, -z$.

Cu3−N3−C3 among the Cu−N_{ax}−C_{ax} angles. The same structural diversity of L is observed in **3**. The six lattice water molecules in the unit cell undergo hydrogen bonding to each other and/or OH groups of L, and two among them are also hydrogen-bonded to terminal CN ligands. Furthermore, the remaining noncoordinated CN groups are subject to hydrogen bonds to secondary amines. Thus, the hydrogen bonds between OH and secondary amines or/and water molecules play a crucial role in crystallizing and stabilizing the structures of **2** and **3** since the use of methyl and ethyl pendent groups instead of the hydroxyl groups provided no crystalline products in this system.

As displayed in Figure 3, the extended structure of **2** in the *bc* plane can be represented as a 2D honeycomblike layer, which is reminiscent of those of hexacyanometalate-based bimetallic assemblies.[26] The edge distances between M atoms in an irregular hexagon range from 10.818 to 11.535 Å for **2** and from 10.876 to 11.580 Å for **3**. The Cu ions lie right on the *bc* plane while the M centers are placed alternately upside and downside of the same layer. As seen in Figure 4, the layers are packed together along the *a*-axis with the shortest interlayer separations of 7.333 Å for Mo−Cu, 9.436 Å for Mo−Mo (**2**) and 7.347 Å for W−Cu, 9.022 Å for W−W (**3**).

Magnetic Properties. The temperature dependence of magnetic susceptibility data for **2** and **3** is shown in Figures 5 and 6 in the form of $\chi_m T$ and $1/\chi_m$ versus T. The $\chi_m T$ value corresponds to 1.89 cm^3 K mol^{-1} (**2**) and 1.84 cm^3 K mol^{-1} (**3**) at 300 K, which are close to the spin-only one (1.88 cm^3 K mol^{-1}) expected for isolated three Cu(II) ($S_{Cu} = 1/2$) and

(26) (a) Colacio, E.; Domínguez-Vera, J. M.; Ghazi, M.; Kivekäs, R.; Lloret, F.; Moreno, J. M.; Stoeckli-Evans, H. *Chem. Commun.* **1999**, 987. (b) Kou, H.-Z.; Gao, S.; Ma, B.-Q.; Liao, D.-Z. *Chem. Commun.* **2000**, 713.

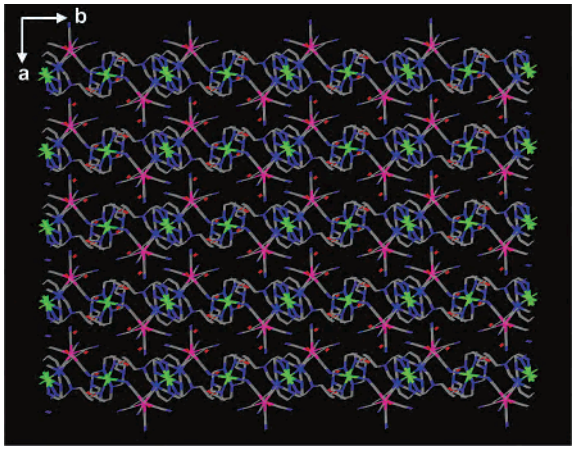

Figure 4. Side view of **2** showing the positions of Cu and Mo atoms in the layer.

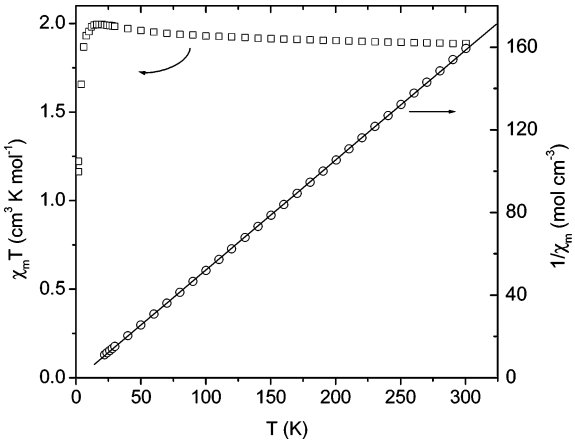

Figure 5. Plots of $\chi_m T$ and $1/\chi_m$ vs T for **2**. The solid line shows the best theoretical fit.

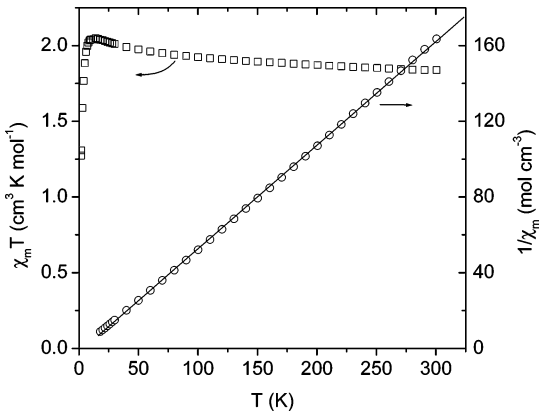

Figure 6. Plots of $\chi_m T$ and $1/\chi_m$ vs T for **3**. The solid line presents the best theoretical fit.

two M(V) ($S_M = 1/2$) ions. As temperature is lowered, $\chi_m T$ experiences a gradual rise and reaches a maximum value of 2.00 cm^3 K mol^{-1} at 18 K for **2** and 2.05 cm^3 K mol^{-1} at 14 K for **3**. This behavior indicates the existence of ferromagnetic interactions between magnetic centers. A sharp drop below the cusp temperature is observed, designating that prevalent antiferromagnetic couplings in both complexes are operative. In the temperature range 18−300 K, the inverse magnetic susceptibility data were fitted with the Curie−Weiss law, affording parameters of $C = 1.88$ cm^3 K mol^{-1},

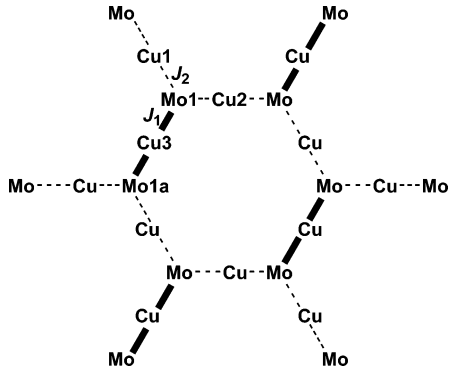

Figure 7. Magnetic exchange model of **2** in which the thick solid lines stand for interactions (J_1) through the rather linear M−CN−Cu route and the thin dotted ones are considered as magnetic couplings (J_2) via the more bent M−CN−Cu pathway.

$\Theta = 2.0$ K for **2** and $C = 1.83$ cm^3 K mol^{-1}, $\Theta = 3.9$ K for **3**. The positive Weiss constant (Θ) demonstrates that neighboring Cu(II) and M(V) spins in the lattice are coupled ferromagnetically.

Two plausible magnetic pathways through the CN bridges exist: one is through the rather linear route (J_1) of M−CN−Cu with the Cu−NC angle of around 160°, and the other is via the more bent linkage (J_2) with the Cu−NC angle of below 144° (Figure 7). Additionally, the bond distance of Cu−N_{ax} for J_1 is shorter by ∼0.02 Å than that for J_2. In case of the magnetic pathway (J_1) of Mo−CN−Cu, with the Cu−N_{ax} bond length of 2.548 Å and Cu−NC(Mo1) angle of 157.8°, the ferromagnetic nature between Mo(V) and Cu(II) was understood by the fact that the magnetic orbital ($3d_{x^2-y^2}$) on the Cu(II) atom oriented toward four equatorial N atoms of L is not effectively delocalized on the empty π^* orbitals of the CN bridges, due to the long bond distances that generate the π-overlap with the orbitals ($5d_{z^2}$:$5d_{x^2-y^2}$) of adjacent Mo(V) atoms.[21d,23,24,27] Therefore, the total exchange coupling constant (J_1), contributed from ferromagnetic ($J_{1F} > 0$) and antiferromagnetic ($J_{1AF} < 0$) components, becomes positive because J_{1AF} proportional to overlap integral is virtually zero under the aforementioned structural environment. For the other magnetic pathway (J_2), provided that the Cu−NC(Mo1) angle turns more bent without varying the Cu−N_{ax} distance too much, the magnetic orbitals start to overlap and the J_{2AF} contribution would not be ruled out, probably leading to a negative J_2, which will be discussed below. However, there is no proper theoretical expression to explain the 2D spin exchange interaction of these type of compounds so that it is not possible to extract from a magnetic fitting process exchange coupling constants (J_1 and J_2) between Cu(II) and M(V) magnetic centers.

As seen in Figures 8 and 9, the field dependence of the magnetization shows that the magnetization curve at 1.9 K increases with raising applied field but its value surprisingly stays smaller than the theoretical value calculated from the Brillouin function for uncoupled three Cu(II) and two M(V) spins. Such behavior may suggest that ferromagnetic interactions ($J_1 > 0$) coexist with antiferromagnetic couplings ($J_2 < 0$) in the 2D structure. This explanation is ascertained by the fact that the maximum of the $\chi_m T$ values (2.00 cm^3 K mol^{-1} at 18 K for **2** and 2.05 cm^3 K mol^{-1} at 14 K for **3**) is smaller than the theoretical expected values (2.63 cm^3 K mol^{-1} for the ferromagnetic trimer CuM_2 (J_1) through the linear CN bridge and two isolated paramagnetic Cu ions), demonstrating that a M(V) spin in the trimer is antiferromagnetically coupled with the paramagnetic Cu(II) spins via the bent CN linkage (J_2).[19b] For **2**, the data points at 20 K go on a rise faster than the calculated curve, indicating that dominant ferromagnetic interactions are present, which well supports the ferromagnetic nature at 20 K, as shown in Figure 5. The analogous behavior found at 14 K for **3** supports the presence of ferromagnetic couplings at the given temperature.

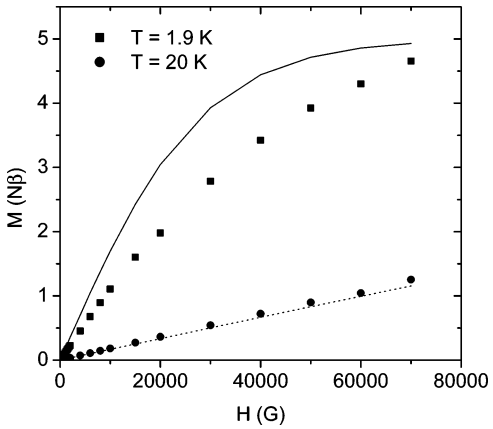

Figure 8. Field dependence of the magnetization of **2**. The solid and dotted lines illustrate the Brillouin curves for independent three Cu(II) and two Mo(V) ions at 1.9 and 20 K, respectively.

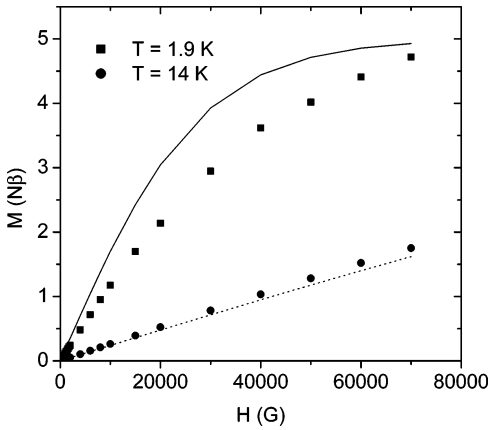

Figure 9. Field dependence of the magnetization of **3**. The solid and dotted lines describe the Brillouin curves for isolated three Cu(II) and two W(V) ions at 1.9 and 14 K, respectively.

Conclusions

We have prepared a new macrocyclic Cu(II) (**1**) complex, which was employed as a molecular precursor to construct magnetic bimetallic systems with higher dimensionality. Self-assembling the precursor and octacyanometalates(V) resulted in two cyano-bridged 2D layered $Cu^{II}-M^{V}$ (M = Mo(**2**), W(**3**)) bimetallic compounds with novel honeycomblike structures, which marks the first structural patterns found in octacyanometalate(V)-based bimetallic systems. Interestingly,

(27) Hendrickx, M. F.; Mironov, V. S.; Chibotaru, L. F.; Ceulemans, A. *Inorg. Chem.* **2004**, *43*, 3142.

three types of molecular arrangements in the macrocycle L, which are generated with assistance of hydrogen bonds to their neighbors, are observed within the crystal lattice. They play a central role in determining structural parameters, especially bond angles of the surrounding $Cu-N_{ax}-C_{ax}$ units, which are regarded as magnetically essential structural factors. The magnetic measurements reveal that ferromagnetic and antiferromagnetic couplings occur between Cu^{II} and $Mo^{V}(W^{V})$ centers through the CN bridges.

Acknowledgment. This work is financially supported by the CRM-KOSEF. C.S.H thanks the Operation Program on Shared Research Equipment of KBSI and MOST.

Supporting Information Available: Crystallographic information in CIF format. This material is available free of charge via the Internet at http://pubs.acs.org.

IC050634C